

Crystal Growth and Structure Determination of Pigment Orange 82

Martin Kaiser,^[a] Aron Wosylus,^[b] Birgit Gerke,^[c] Rainer Pöttgen,^[c] Karel Prokeš,^[d] Michael Ruck,^[a, e] Thomas Doert,^{*[a]}

In memoriam Dr. Norbert Mronga.

Abstract: The crystal structure of the important industrial orange pigment PO82, major part of the BASF Colors & Effects® product Sicopal® Orange K/L 2430, was solved from combined X-ray single crystal, X-ray and neutron powder diffraction, ¹¹⁹Sn Mössbauer spectroscopy, transmission electron microscopy, electron diffraction, and chemical analyses. The structure contains Keggin type clusters composed of four [M₃O₁₃] trimers consisting each of three MO₆ octahedra that share edges and one common oxygen atom connecting the trimers to the central ZnO₄ tetrahedron. The octahedrally coordinated metal atom position is mixed occupied by Ti⁴⁺, Sn⁴⁺ and Zn²⁺. Adjacent Keggin clusters share vertices and are further interconnected to four ZnO₄ tetrahedra. This framework of interconnected MO₆ octahedra and ZnO₄ tetrahedra contains channels along [110] in which the Sn²⁺ cations are located.

Introduction

In the industrial orange-red color space only a few lead-free inorganic pigments are available at reasonable costs. Mentionable are iron oxides and hydroxides, metal sulfides, CICIP (Complex Inorganic Color Pigments), and the here investigated TiO₂–ZnO–SnO based products.^[1] Titanium-zinc-tin oxide based pigments are available from different suppliers like Shepherd under name Shepherd Orange 10P340, from Venator called Solaplex® Bright Orange 34H1004, and from BASF under the trade name Sicopal® Orange K/L 2430 for both, paint and plastic applications.

A pigment on titanium-zinc-tin oxide based basis was first patented in 1983 by Johnson Matthey.^[2] Subsequent

developments by BASF showed, that the addition of other metal oxides, like rare earths or alkaline metal oxides, improve its color properties.^[3] However, the crystal structure of the main ingredient and color determining phase Pigment Orange 82 remained unknown. Here we report on this structure, which was solved in a combined diffraction and spectroscopic study. With respect to its main structural building unit, we name this phase *kegginite B*, where B stands for BASF.

Results and Discussion

The industrial product Sicopal® Orange K/L 2430, supplied by BASF Pigments GmbH, Besigheim, Germany, was used as starting material for structure analysis. The product generally consists of the orange pigment PO82, which is a ternary Zn-Ti-Sn oxide (later on referred to as kegginite B), TiO₂ (rutile), and admixtures of a spinel phase with the composition TiZn₂O₄, as evidenced by X-ray powder data (PXRD, Figure S1).

To obtain crystals suitable for structure analysis the industrial sample was re-annealed in an alumina crucible enclosed in an evacuated silica tube at $T = 1170$ K for one week. Notably, Zn₂SiO₄ formed at the walls of the fused silica ampoule indicating that the gas phase contains a certain amount of ZnO during the heat treatment. This goes along with a decrease of the by-product TiZn₂O₄ as evidenced by X-ray powder data (Figure S1). Further annealing of the remaining orange intermediate at $T = 1220$ K for 6 days followed by slow cooling (–6 K/h to 920 °C and –30 K/h to 895 °C) resulted in an essentially two-phase sample, namely the orange phase kegginite B, and rutile (see Figure S1). Small, intensely orange-colored crystals were selected for single-crystal diffraction experiments. EDS measurements on several of these crystals showed a Sn-rich atomic ratio compared to the as-received material (Tables S1 and S2), consistent with the observed loss of ZnO. In contrast, the average composition of the two-phase sample remained nearly identical to the pristine sample according to chemical analyses of the bulk material (detailed results are given in Table S2); no nitrogen was found above the detection threshold (0.05 wt.-%), see below.

During attempts to prepare several grams of the material for neutron diffraction experiments in alumina crucibles applying the same heat treatment, the same phase separation was observed. This sintering procedure yielded compact rods (Figure 1) with the orange colored phase re-crystallized at the surface forming an area of larger, intensely red-colored crystals besides a zone of loosely sintered particles. The latter showed the typical orange color (Figure 1, right) and the PXRD of industrial sample (Figure S1). The grayish bottom end of the rods consisted of TiO₂

* Prof. Dr. Th. Doert

E-mail: thomas.doert@tu-dresden.de

[a] Dr. M. Kaiser, Prof. Dr. M. Ruck, Prof. Dr. Th. Doert
Fakultät Chemie und Lebensmittelchemie, Technische Universität
Dresden, 01062 Dresden, Germany

[b] Dr. A. Wosylus
BASF Pigment GmbH
74354 Besigheim, Germany

[c] Dr. B. Gerke, Prof. Dr. R. Pöttgen
Institut für Anorganische und Analytische Chemie, Universität
Münster, Corrensstrasse 30, 48149 Münster, Germany

[d] Dr. K. Prokeš
Helmholtz-Zentrum Berlin für Materialien und Energie, M-ICMM,
Hahn-Meitner Platz 1, 14109 Berlin, Germany

[e] Prof. Dr. M. Ruck
Max Planck Institut für Chemische Physik fester Stoffe
Nöthnitzer Str. 40, 01187 Dresden, Germany

Supporting information for this article is given via a link at the end of the document.

(Figure 1, left; Figure S3). Similarly to the selected crystals, the orange-colored powder is slightly richer in tin as compared to the as-received material: Sn : Zn : Ti : O = 1.5 : 1.0 : 1.6 : 6.9 according to chemical analyses (Table S2). Only the Sn-rich orange-colored fraction of the rod was used for the neutron diffraction experiment.



Figure 1. Re-annealed product obtained after the heat-treatment of Sicopal® Orange K/L 2430, at 950 °C. A phase separation into larger crystals of the PO82 and gray TiO₂ is observed at the bottom of the sintered powder rod.

Single Crystal Structure Determination

Powder and single-crystal diffraction data of the orange pigment phase can be indexed in a cubic *F*-centered lattice with $a = 14.8793(7)$ Å ($T = 100$ K, X-ray powder data). Reflection conditions are compatible with the non-centrosymmetric space group $F\bar{4}3m$ (no. 216). The cubic symmetry and the approximate lattice parameter of the pigment phase were also confirmed by selected area electron diffraction (SAED) patterns recorded on crystallites of the industrial sample.

Several single-crystals of the annealed material were investigated. They showed the same diffraction patterns and essentially the same lattice parameters within experimental errors. However, the crystal quality differed very much judged on broad reflections and diffuse scattering contributions. A suitable single-crystal was used for a full data collection at $T = 100$ K.

Setting up a crystallographically accurate and chemically meaningful structure model was not possible from X-ray diffraction data alone. Instead, additional information (chemical analyses, neutron diffraction and Mössbauer spectroscopy, e.g.) had to be considered and partly to be incorporated in the structure model as constraints. As we deal with a colored oxide, the structure model should be electron precise and the structure-chemical discussion is based on an ionic description considering classical oxidation states for all atoms.

The initial structure solution yielded two tetrahedral MO_4 , one distorted octahedral MO_6 , and one square pyramidal MO_4 coordination polyhedra with different electron densities on the *M* sites. Besides, one disordered and significantly less occupied metal position was deduced from the Fourier maps that also needed to be taken into consideration.

To start with the most obvious, two regular MO_4 tetrahedra with *M*-O distances of $4 \times 1.937(3)$ Å (metal atom on Wyckoff site 4*d*) and $3 \times 1.950(2)$ Å and $1 \times 1.951(1)$ Å (Wyckoff site 16*e*) were found (Figure 2, B and C). The interatomic distances in these MO_4 tetrahedra correspond to typical Zn–O distances (e.g., 1.980 Å – 2.005 Å in wurtzite-type ZnO).^[4] The refinement of the respective atom positions (Wyckoff sites 4*d* and 16*e*) with zinc converged smoothly without significant residual electron density.

The metal on a third position (Wyckoff site 24*g*) is coordinated by four oxygen atoms on one side of the metal atom only, forming a slightly distorted square MO_4 pyramid with the metal atom at the apical position (Figure 1, D, atom Sn1). The *M*-O distances are $2 \times 2.193(2)$ Å and $2 \times 2.353(2)$ Å, respectively. Both, *M*-O distances and the shape of the metal coordination sphere are indicative for tin(II) with a 5s lone pair in accordance with literature data (black SnO, romarchite: 4×2.224 Å;^[5] red SnO: 2.038 Å – 2.670 Å).^[6] The refinement of the metal site (Wyckoff position 24*g*) converged well and the difference Fourier ($F_o - F_c$) map around the Sn1 position was featureless, hence.

A considerable electron density maximum of $16 \text{ e}/\text{Å}^3$ was found in the difference Fourier map at 0.07, 0.07, 0.10 (Wyckoff site 48*h*). The coordinates are close to the threefold rotation axis in *x, x, x*, which means, that three crystallographically equivalent positions exist within a distance of 0.75 Å to each other, of which only one can be occupied. Because the electron density at this position is too high for a 3*d* transition metal atom, a disordered tin position was considered (Figure 2, D, atom Sn2). According to the asymmetric three-fold coordination by oxygen, the valence state of tin should be +II, too. The occupancy of this disordered Sn2 position converged to 0.21 or about 10 additional tin(II) atoms per unit cell.

Uncertainty of the element assignment arises from the distorted MO_6 octahedron with *M*-O distances of 1.882(1) Å, $2 \times 1.942(2)$ Å, $2 \times 2.023(2)$ Å and 2.071(3) Å; (*M* on Wyckoff site 48*h*; Figure 2, E). This octahedral position seems to be suitable for titanium(IV) as the average *M*-O distance of 1.981(2) Å accords well with that of rutile (2×1.980 Å, 4×1.949 Å)^[7]. The integrated number of electrons in the octahedral void is ca. 26 and does, thus, not fit with the scattering contribution of titanium alone, but indicates the contribution of a heavier atom, most likely tin, on a mixed occupied site. The oxidation state of tin should be +IV here, as the stable modification of SnO₂ (cassiterite) adopts the rutile structure with Sn–O distances of 2×2.056 Å and 4×2.052 Å.^[8] Moreover, the substitution of titanium(IV) by tin(IV) in rutile is known.^[9] ¹¹⁹Sn Mössbauer spectroscopy provides clear evidence for the presence of tin(IV) besides tin(II) in the re-annealed samples and suggest a tin(II) : tin(IV) ratio of 83 : 17 (see below).

From this ratio and the occupancies of the tin(II) sites (34 Sn²⁺ atoms per unit cell) 7 tin(IV) atoms and a total tin content of 41 atoms per unit cell result. This would translate into tin(IV) and titanium(IV) occupancies of ca. 0.15 and 0.85 for the octahedral site, which satisfactorily approximates the observed electron density. However, this does not result in a charged-balanced model, but in an excess of 20 positive charges per unit cell. Moreover, a significant zinc shortfall (Sn : Zn : Ti = 40 : 20 : 40 = 1.6 : 0.8 : 1.6) with respect to results of EDS (Sn : Zn : Ti = 40(3) : 25(3) : 35(2) at.-%) and chemical analyses (Sn : Zn : Ti : O = 1.5 : 1.0 : 1.6) is calculated (Table S1 and S2).

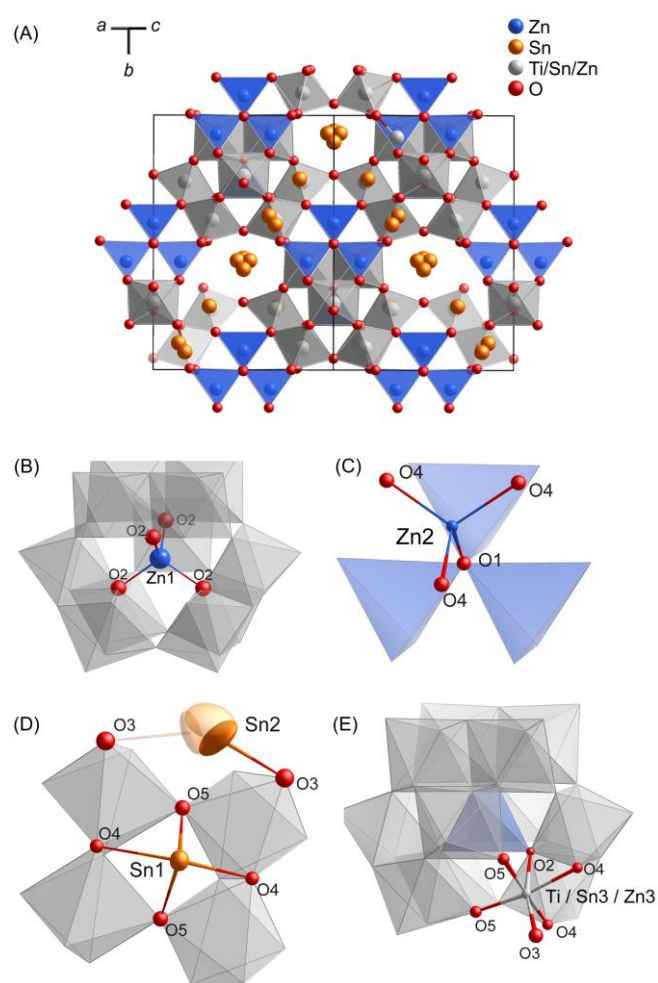


Figure 2. Crystal structure of kegginite B (A) Zn coordination sphere of the Zn atoms (B and C), the Sn^{2+} atoms (D), and the mixed occupied octahedral site containing about 70 at.-% Ti^{4+} , 15 at.-% Sn^{4+} , and 10 at.-% Zn^{2+} (E). The ellipsoids drawn in (B)–(E) represent 90 % probability.

As chemical analyses and neutron diffraction experiments provided no evidence for other anions than oxide, charge balancing by nitride, can be excluded. No hints for vacancies or low occupancies were observed for the tetrahedral zinc sites and for the tin(II) site 24g (Sn1), so that only the occupancy of the octahedral voids remains an option to achieve a charge-balanced structure model that matches the chemical analysis as well as the electron density within the limitations of the applied methods.

To reflect the analytically determined metal ratios, the octahedral 48h position was treated as mixed occupied by titanium, tin, and zinc which were refined with one set of anisotropic displacement parameters. A charge-balanced final structure model was achieved by allowing also voids on the octahedral site. Therefore, the refinement needed several initial restrictions for site occupancies, atomic coordinates and displacement parameters. The tin(IV) occupancy was set by the tin(II) : tin(IV) ratio of 83 : 17 as stated before. A second constraint

was applied to the zinc(II) occupancy on the 48h position to make sure that the combination of voids, di- and tetravalent cations lead to a charge balanced structure model. The occupancy of titanium could then be refined without further restrictions; the oxygen atoms were restricted to individual isotropic displacement parameters.

The model finally converged to residual values of $wR_2 = 0.062$, a goodness-of-fit of 1.05, and a featureless Difference Fourier map. The results of this refinement as well as some basic crystallographic parameters are listed in Table 1. Selected atomic parameters as well as interatomic distances are given in the Supporting Information (Table S3 - S5).

Table 1. Crystallographic data for kegginite B at $T = 100(2)$ K.

Sum formula	$\text{Sn}_{10.32(3)}\text{Zn}_{6.14(7)}\text{Ti}_{8.39(4)}\text{O}_{35}$
Crystal system, space group	cubic, $F\bar{4}3m$ (no. 216)
Lattice parameter	$a = 14.8793(7)$ Å,
Formula units per cell	$Z = 4$
Calculated density	$\rho_{\text{calc.}} = 5.22$ g cm^{-3}
Range for data collection; Index ranges; collected reflections	$4.74^\circ \leq 2\theta \leq 79.96^\circ$ ($\lambda = 0.71073$ Å); $-26 \leq h \leq 17$, $-25 \leq k \leq 26$, $-26 \leq l \leq 26$; 16292 measured; 1059 unique
R indices of data merging	$R_{\text{int}} = 0.051$, $R_\sigma = 0.021$
Structure Refinement	Full-matrix least-squares based on F^2 , inversion twin, twin ratio 0.48(3) : 0.52(3)
Data / constraints / parameters	1059 / 2 / 35
Final R indices and Goodness-of-fit on F^2	$R_1[924 I > 3\sigma(I)] = 0.027$ $wR_2(\text{all } F_o^2) = 0.063$ $\text{Goof} = 1.10$
Min./max. residual electron density	$-1.55 / 2.22$ e \AA^{-3}

The relative amounts of Sn3, Zn3, and Ti on the octahedral position refined to 0.1463(5), 0.095(6), and 0.699(3), respectively. The overall metal ratio of the structure model (Sn : Zn : Ti = 42 : 25 : 34 at.%) accords well with the EDS measurements on several crystals (Sn : Zn : Ti = 40(3) : 25(3) : 35(2) at.-%, Table S1). We attribute the slightly higher amount of titanium in the chemical analysis of the bulk to traces of TiO_2 , which is a by-product of the re-annealing process.

The structure of the kegginite B pigment, $\text{Sn}_{10.32(3)}\text{Zn}_{6.14(7)}\text{Ti}_{8.39(4)}\text{O}_{35}$, is a three-dimensional oxometalate framework. About 0.7 Titanium(IV), 0.15 tin(IV), and 0.1 zinc(II) share statistically the site in MO_6 octahedra of zinc centered Keggin clusters (Figure 2B and 1E),^[10-12] which lead us to the name kegginite B. These Keggin clusters are composed of four $[\text{M}_3\text{O}_{13}]$ trimers consisting each of three MO_6 octahedra that share edges and one common oxygen atom (O2) located on the threefold axis. This oxygen atom connects the $[\text{M}_3\text{O}_{13}]$ trimers to the tetrahedrally coordinated central zinc(II) atom (Zn1). The

ARTICLE

Keggin clusters have T_d symmetry and can thus be labelled to belong to the α isomer series.^[11] They share vertices (O3) with neighboring Keggin clusters and are further interconnected via the O4 oxygen atoms to four ZnO_4 tetrahedra (Zn2) that are arranged similar to the motif found in IR-MOFs.^[13] This framework of interconnected MO_6 octahedra and ZnO_4 tetrahedra contains channels along [110], in which the Sn2 atoms are located, Figure 2A.. While Sn1 atoms are connected to four MO_6 octahedra of two different $[M_3O_{13}]$ trimers, the Sn2 atoms are found slightly off the three-fold axis between the SnO_4 pyramids of Sn1, Figure 2D.

Powder X-ray and neutron diffraction

The final structure model was confirmed by Rietveld analyses on X-ray as well as neutron diffraction data applying the same set of constraints for the occupancies in the octahedral site. The X-ray powder as well as the neutron powder diffraction patterns and the respective Rietveld fits are depicted in Figure 3 and Figure 4, respectively. Both refinements converge without significant residual intensities in the difference plots (Table 3). However, the occupancies of the disordered sites differ from the single-crystal structure determination and vary on the different samples (PXRD: Sn2: 0.284(3), Sn3: 0.1606(6), Zn3: 0.27(1), Ti: 0.563(7); neutron diffraction: Sn2: 0.12(2), Sn3: 0.127(3), Zn3: 0.03(3), Ti: 0.80(1)), which might be indicative of a certain phase width.

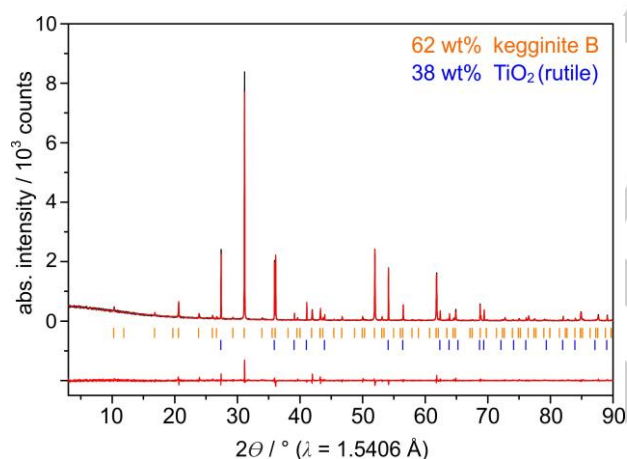


Figure 3. PXRD pattern (black) and Rietveld fit (red) of a re-annealed sample of commercial Sicopal[®] Orange K/L 2430, consisting of a mixture of the orange pigment kegginites B (62(2) wt.-%) and TiO_2 (rutile type, 38(2) wt.-%). Possible substitution of the Ti site by Sn atoms was not considered for the rutile phase (cf. text for details).

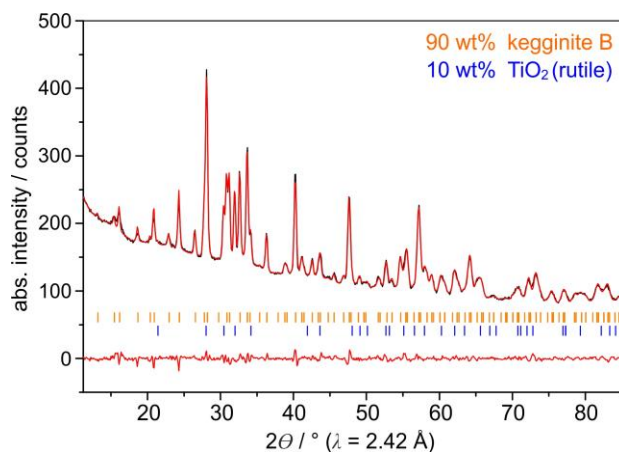


Figure 4. Neutron diffraction pattern (black) and Rietveld fit (red) of a re-annealed sample of commercial Sicopal[®] Orange K/L 2430, consisting of a mixture of the orange pigment kegginites B (90(6) wt.-%) and TiO_2 (rutile type, 10(6) wt.-%). Possible substitution of the Ti site by Sn atoms was not considered for the rutile phase (cf. text for details).

¹¹⁹Sn Mössbauer spectroscopy

The ¹¹⁹Sn spectra of the re-annealed commercial product at room temperature and $T = 78$ K are presented in Figure 5 along with transmission integral fits. The corresponding fitting parameters are listed in Table 2. The spectra are almost the same at the two temperatures. The largest difference concerns the slight asymmetry of the quadrupole split Sn(II) signal at room temperature. In the following we rely on the 78 K data. The spectrum was well reproduced with a superposition of a tin(II) ($\delta = 3.06(1)$ mm·s⁻¹) and a tin(IV) ($\delta = -0.10(1)$ mm·s⁻¹) signal. The isomer shift of the tetravalent tin atoms is similar to the one of cassiterite, SnO_2 of 0 mm·s⁻¹.^[14-16] We observed only weak quadrupole splitting with $\Delta E_Q = 0.45(1)$ mm·s⁻¹, and the experimental line width parameter of $\Gamma = 0.78(2)$ mm·s⁻¹ is in the usual range.

The divalent tin atoms show a higher isomer shift of $\delta = 3.06(1)$ mm·s⁻¹ as compared to binary SnO (2.7 mm·s⁻¹),^[14-16] indicating slightly higher s-electron density at the tin nuclei. The higher quadrupole splitting parameter of $\Delta E_Q = 1.70(1)$ mm·s⁻¹ is a consequence of the tin(II) lone pair character (asymmetric distribution of electron density). Integration of the tin(II) and tin(IV) signals lead to an atomic ratio of 83(1) : 17(1).

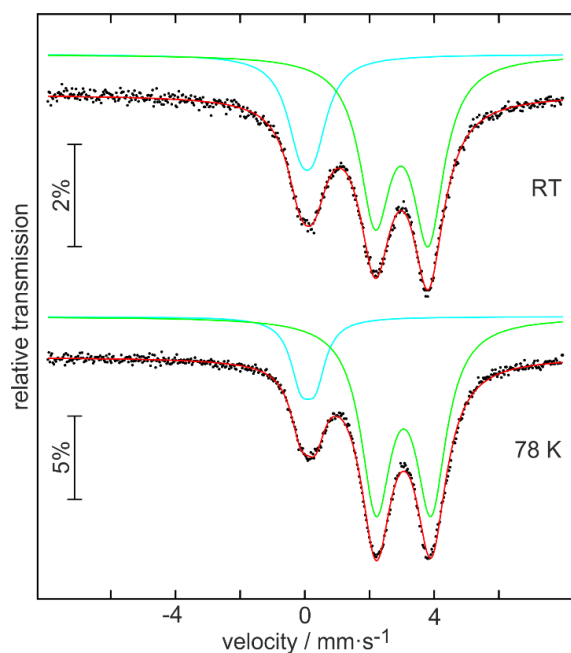


Figure 5. Experimental (data points) and simulated (continuous lines) ^{119}Sn Mössbauer spectra of a re-annealed sample of Sicopal® Orange K/L 2430 at room temperature and 78 K.

Table 2. Fitting parameters of ^{119}Sn Mössbauer spectra of a re-annealed sample of Sicopal® Orange K/L 2430 at ambient temperature and at $T = 78\text{ K}$; δ = isomer shift, ΔE_Q = electric quadrupole splitting, Γ = experimental line width, A_{21} = asymmetry of the quadrupole split signal. The color code of the subspectra is also indicated. Parameters marked with an asterisk were kept fixed during the final fitting procedure.

signal	δ ($\text{mm}\cdot\text{s}^{-1}$)	ΔE_Q ($\text{mm}\cdot\text{s}^{-1}$)	Γ ($\text{mm}\cdot\text{s}^{-1}$)	ratio (at.-%)	A_{21}
ambient temperature:					
tin(II) (green)	3.00(1)	1.64(1)	1.18(1)	73(1)	1.12(1)
tin(IV) (blue)	-0.07(1)	0.44(2)	1.03(2)	27(1)	1*
$T = 78\text{ K}$:					
tin(II) (green)	3.06(1)	1.70(1)	1.14(1)	83(1)	1*
tin(IV) (blue)	-0.10(1)	0.45(1)	0.78(2)	17(1)	1*

Conclusions

A structure model of the main phase of the industrial pigment BASF Colors & Effects® Sicopal® Orange K/L 2430 was established by a combination of single-crystal and powder X-ray diffraction, powder neutron diffraction, ^{119}Sn Mössbauer spectroscopy, transmission electron microscopy and chemical analyses. The most striking structural building unit is a ZnO_4 -centered α -Keggin cluster – leading us to call this phase kegginite

B – besides corner sharing ZnO_4 tetrahedra and Sn(II)O_4 tetragonal pyramids. The octahedral metal sites of the Keggin cluster are mixed occupied Ti(IV) , Sn(IV) and additional Zn(II) for charge balancing. Kegginite B, thus, is a mixed-valent phase containing Sn(II) and Sn(IV) as evidenced by ^{119}Sn Mössbauer spectroscopy.

Experimental Section

Sample preparation. Commercial grade Sicopal® Orange K/L 2430 provided by BASF was used as starting material. According to powder X-ray diffraction data and SEM/EDX analyses, this sample contained a mixture of the actual orange pigment with TiO_2 (rutile type) and TiZn_2O_4 (spinel type). In order to facilitate crystal growth, the sample was placed in alumina crucibles and annealed at $T = 1173\text{ K}$ for one week. After a second annealing at $T = 1223\text{ K}$ for 6 days the resulting mixture of the orange pigment and TiO_2 (rutile type) was slowly cooled (-6 K/h to 1193 K and -30 K/h to 1168 K). Note that partial phase separation was observed during the annealing. The orange colored fraction of the annealed sample has also been used for X-ray and neutron diffraction experiments and ^{119}Sn Mössbauer spectroscopy.

Elemental analysis. For the elemental analysis of Ti, Zn, Sn, O and N combinations of different methods were used. The analysis of the metallic elements was done by inductively coupled plasma atomic emission spectroscopy using a 5100 SVDV (Agilent). The oxygen and nitrogen contents were probed with the carrier gas hot extraction method using a TCH 600 (LECO). The results of the chemical analyses of the pristine and the re-annealed samples are given in Table S2.

Scanning electron microscopy and energy dispersive X-ray analysis.

The samples were fixed on a sample holder with a graphite pad. Scanning electron microscopy (SEM) was performed by using a SU8020 instrument (Hitachi) with a triple detector system for secondary and low-energy backscattered electrons ($U_e = 3\text{ kV}$). The compositions of the samples were determined by quantitative energy dispersive X-ray spectroscopy (EDS, $U_e = 20\text{ kV}$) analysis using a Silicon Drift Detector X-Max^N (Oxford). In light of the preparation method, the elements C and O (both part of the polymer) were omitted in EDS quantifications.

Samples for **transmission electron microscopy (TEM)** were prepared on ultra-thin carbon TEM carriers. The samples were imaged by TEM using a Tecnai Osiris machine (FEI Company, Hillsboro, USA) operated at 200 keV under bright-field as well as high-angle annular dark-field scanning TEM (HAADF-STEM) conditions. Chemical composition maps were acquired by energy-dispersive X-ray spectroscopy (EDXS). Images and elemental maps were evaluated using the iTEM (Olympus, Tokyo, Japan, version: 5.2.3554) as well as the Esprit (Bruker, Billerica, USA, version 1.9) software packages.

Samples for **electron probe microanalysis (EMPA)** were fixed on a carrier substrate using conducting carbon paste. EMPA was conducted on a JSM-7500-TFE (Jeol, Tokyo, Japan) machine.

Single-crystal X-ray diffraction. Single-crystal experiments were performed on a Bruker Kappa Apex II CCD diffractometer with $\text{Mo-K}\alpha$ radiation using the software package Apex Suite.^[17] Two crystal domains were identified and separated after integration. A numerical absorption correction based on an optimized crystal description^[18] was applied in JANA2006.^[19] The initial structure solution was performed using the charge flipping algorithm.^[20] Diamond 4 was used for structure visualization.^[21] Further details on the crystal structure investigations can

be obtained from the Fachinformationszentrum Karlsruhe, 76344 Eggenstein-Leopoldshafen, Germany (fax: (+49)7247-808-666; e-mail: crysdata@fiz-karlsruhe.de), on quoting the depository numbers CSD-1883455.

Powder X-ray diffraction. Powder X-ray diffraction (PXRD) was performed at 296(1) K on an X'Pert Pro MPD diffractometer (PANalytical) equipped with a curved Ge(111) monochromator by using Cu-K α_1 radiation ($\lambda = 1.54056$ Å). Le Bail analyses and Rietveld fits were done with Jana 2006.^[19]

Powder neutron diffraction. The powder neutron diffraction experiment was performed on the instruments E1 and E2 at the BER II reactor of the Helmholtz-Zentrum Berlin (HZB). Fine powder was placed in a vanadium sample holder and investigated at room temperature. The E1 instrument is a standard triple-axis spectrometer using Soller type collimators and a single ^3He detector with a high efficiency. The flat-cone E2 diffractometer utilizes a set of four 30×30 cm 2 position sensitive ^3He detectors with a radial oscillating collimator in front of them. While on the instrument E1 we used a pyrolytic graphite monochromator selecting the wavelength $\lambda = 2.42$ Å, on the instrument E2 that offers a better resolution of 15', we have used a Ge-monochromator selecting the neutron wavelength $\lambda = 1.21$ Å. On E1 the powder patterns were recorded in a step by step elastic mode with two different collimators (20' and 40') in the range $10^\circ \leq 2\theta \leq 75^\circ$, where 2θ denotes the scattering angle for about two hours each. On E2 we have collected data in the range $6.7^\circ \leq 2\theta \leq 87.8^\circ$ for about 19 hours. The Rietveld refinements of the neutron diffraction data were carried out with JANA2006.^[19]

Table 3. Crystallographic data for kegginite B from Rietveld refinements of X-ray powder as well as the neutron powder diffraction data.

	X-ray diffraction	Neutron diffraction
Crystal system, space group	cubic, $F\bar{4}3m$ (no. 216)	
Sum formula, formula units	$\text{Sn}_{11.34(4)}\text{Zn}_{8.2(2)}\text{Ti}_{6.76(8)}\text{O}_{35}$, $Z = 4$	$\text{Sn}_{9.0(2)}\text{Zn}_{5.4(4)}\text{Ti}_{9.6(1)}\text{O}_{35}$, $Z = 4$
Lattice parameter	$a = 14.93741(5)$ Å,	$a = 14.914(1)$ Å,
Calc. density	5.5 g cm $^{-3}$	4.9 g cm $^{-3}$
Range for data collection	$3^\circ \leq 2\theta \leq 90^\circ$; $\Delta(2\theta) = 0.013^\circ$ ($\lambda = 1.5406$ Å); 6690 data points	$11.2^\circ \leq 2\theta \leq 85.7^\circ$; $\Delta(2\theta) = 0.1^\circ$ ($\lambda = 1.211$ Å); 746 data points
Data (all phases) / constraints / parameters	203 reflections / 2 / 15	323 reflections / 2 / 31
Final R indices	$R_p = 0.075$; $wR_p = 0.112$ R_{bragg} (kegginite) = 0.056 $\chi^2 = 1.24$	$R_p = 0.014$; $wR_p = 0.019$ R_{bragg} (kegginite) = 0.020 $\chi^2 = 2.3$

^{119}Sn Mössbauer spectroscopy. A Ca $^{119\text{m}}\text{SnO}_3$ source was used for the ^{119}Sn Mössbauer spectroscopic investigations. The sample was placed within thin-walled PMMA containers at a thickness of about 10 mg Sn/cm 2 . A palladium foil of 0.05 mm thickness was used to reduce the tin-K X-rays concurrently emitted by this source. The measurements were conducted in the usual transmission geometry at room temperature and 78 K with a total counting time of 2 d each. Fitting of the spectra was performed with the Normos-90 program system.^[22]

Acknowledgements

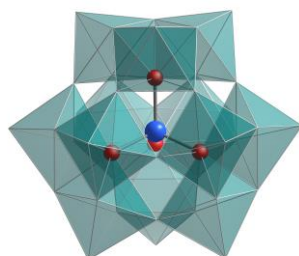
We thank *Dr. M. Reehuis* and *Dr. J.-U. Hoffmann* from HZB for technical help during measurement on E2. *Dr. G. Auffermann*, MPI CPFS Dresden, for the chemical analyses, *Dr. P. Müller*, *U. Flörchinger* and *F. Spindler*, BASF, are acknowledged for TEM measurements and *P. Damm*, *J. Oswald* and *C. Kujat*, BASF, are acknowledged for valuable discussion.

Keywords: pigment • Keggin cluster • structure determination • neutron diffraction • Mössbauer spectroscopy

- [1] G. Buxbaum, *Industrial Inorganic Pigments*, VCH, Weinheim, **1993**.
- [2] J. W. Jenkins, J. Wolstenholme, Colored inorganic complex for use as a pigment and compositions containing it; US patent 4448608, **1983**.
- [3] N. Mronga, K. Bramnik, Colorants comprising tin and rare earth elements, US patent 20100050903, 2007.
- [4] J. Albertsson, S. C. Abrahams, Å. Kvik, *Acta Crystallogr., Sect. B* **1989**, *45*, 34–40.
- [5] J. Pannetier, G. Denes, *Acta Crystallogr., Sect. B* **1980**, *36*, 2763–2765.
- [6] J. Köhler, J. Tong, R. Dinnebier, A. Simon, *Z. Anorg. Allg. Chem.* **2012**, *638*, 1970–1975.
- [7] R. Restori, D. Schwarzenbach, J. R. Schneider, *Acta Crystallogr., Sect. B* **1987**, *43*, 251–257.
- [8] W. H. Baur, *Acta Crystallogr.* **1956**, *9*, 515–520.
- [9] T. Hirata, *J. Am. Ceram. Soc.* **2000**, *83*, 3205–3207.
- [10] G. M. Maksimov, *Russ. Chem. Rev.* **1995**, *64*, 445–461.
- [11] M. T. Pope, A. Müller, *Angew. Chem.* **1991**, *103*, 56–70, *Angew. Chem. Int. Ed. Engl.* **1991**, *30* 34–48.
- [12] M. T. Pope, *Heteropoly and Isopoly Oxometalates*, Springer, Berlin, **1983**.
- [13] M. Eddaoudi, J. Kim, N. Rosi, D. Vodak, J. Wachter, M. O'Keeffe, O. M. Yaghi, *Science* **2002**, *295*, 469–472.
- [14] P. E. Lippens, *Phys. Rev. B* **1999**, *60*, 4576–4586.
- [15] P. G. Harrison (Ed.), *Chemistry of Tin*, Blackie & Son Ltd, Leicester, Great Britain, **1989**.
- [16] P. A. Flinn, Tin Isomer Shifts, in G. K. Shenoy, F. E. Wagner (Eds.), *Mössbauer Isomer Shifts*, North Holland Publishing, Amsterdam, Chapter 9a, **1978**.
- [17] APEX2, Version 2014/9, Bruker AXS Inc., Madison, WI, USA, **2014**.
- [18] X-Shape, Crystal Optimization for Numerical Absorption Correction Program. v. 2.12.2, Stoe & Cie GmbH, Darmstadt, **2009**.
- [19] V. Petříček, M. Dušek, L. Palatinus, *Z. Kristallogr.* **2014**, *229*, 345.
- [20] L. Palatinus, G. Chapuis, *J. Appl. Cryst.* **2007**, *40*, 786–790.
- [21] Brandenburg, K. Diamond 4.5, Crystal Impact GbR, Bonn, **2018**.
- [22] R. A. Brand, Normos, Mössbauer fitting Program, Universität Duisburg, Duisburg (Germany) **2007**.

FULL PAPER

The crystal structure of mixed-valent kegginite B, the main constituent in an important industrial orange pigment, has been established by a combination of diffraction techniques, Mössbauer spectroscopy, electron microscopy, and chemical analyses.

**Keggin clusters**

*M. Kaiser, A. Wosylus, B. Gerke, R. Pöttgen, K. Prokeš, M. Ruck, Th. Doert**

Page No. – Page No.

**Crystal Growth and Structure
Determination of the Orange
Pigment 82**
